

On the Performance of Dual-Antenna Repeater Assisted Bi-Static MIMO ISAC

Anubhab Chowdhury and Erik G. Larsson, *Fellow, IEEE*

Abstract—This paper presents a framework for target detection and downlink (DL) data transmission in a repeater-assisted bi-static integrated sensing and communication system. A repeater is an active scatterer that retransmits incoming signals with a complex gain almost instantaneously, thereby enhancing sensing performance by amplifying the echoes reflected by the targets. The same mechanism can also improve DL communication by mitigating coverage holes. However, the repeater introduces noise and increases interference at the sensing receiver, while also amplifying the interference from target detection signals at the DL users. The proposed framework accounts for these sensing-communication trade-offs and demonstrates the potential benefits achievable through a carefully designed precoder at the transmitting base station. In particular, our finding is that a higher value of probability of detection can be attained with considerably lower target radar-cross-section variance by deploying repeaters in the target hot-spot areas.

Index Terms—Repeater, Integrated sensing and communication, Massive MIMO, GLRT

I. INTRODUCTION

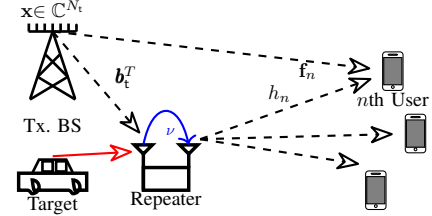
REPEATERS (also known as full-duplex relays) are active scatterers, capable of receiving and retransmitting signals instantly with amplification [1]. They can be deployed on a large scale to enhance coverage for multiple-input multiple-output (MIMO) wireless systems [1]–[6]. Reference [3] demonstrated that repeaters can procure a spectral-efficiency (SE) similar to that of distributed MIMO, while obviating the front-haul signalling overhead. Furthermore, [7] indicated that repeaters can outperform reconfigurable intelligent surface (RIS)-assisted systems, with the additional advantage of repeaters being band/frequency selective. The attractive implementation aspects of repeaters have led to their inclusion in the 5G NR standards since 3rd Generation Partnership Project (3GPP) Release 18 [8].

On parallel avenue, integrated sensing and communication (ISAC) offers efficient spectral and hardware utilization, and is actively being pushed forward as part of 3GPP Release 19, a 5G-advanced/pre-6G initiative [9]. A detailed survey of ISAC is beyond the scope of this paper; readers can refer to [10]–[12] and references therein, and specifically for bi-static ISAC, [13]–[15]. Specifically, [15] optimized RIS-assisted bistatic sensing. The authors in [16] considered repeater-assisted *mono-static* ISAC,¹ where the repeater was

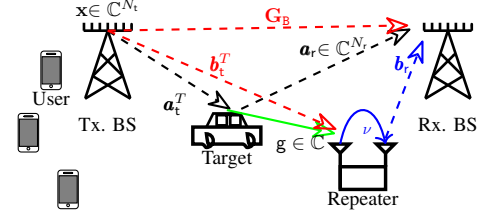
¹The authors are with the Department of Electrical Engineering (ISY), Linköping University, 58183 Linköping, Sweden. Emails: {anuch87, erik.g.larsson}@liu.se

This work was supported in part by the Knut and Alice Wallenberg (KAW) foundation, Excellence Center at Linköping-Lund in Information Technology (ELLIIT), and the Swedish Research Council (VR).

¹In a mono-static setting, the base station (BS) is required to be full-duplex, which in turn incurs additional signal processing and hardware overhead for self-interference cancellation.



(a) Bi-static massive MIMO ISAC: *communication view-point*. Multi-path reflections from the target (not via the repeater) can be incorporated in f_n , which can constitute both line-of-sight (LoS) and non line-of-sight (NLoS) components.



(b) Bi-static massive MIMO ISAC: *sensing view-point*. Clutters are not explicitly drawn to avoid congestion. We neglect the multi-hop reflected channels for the sensing purpose because of the three/multi-fold cascaded path loss effect.

Fig. 1: System model: communication and sensing with a repeater, and its implications to both. Interference links are indicated by red arrows.

used to improve the coverage for DL communication users. In contrast to [16], we investigate the feasibility of *bi-static* ISAC in the presence of a repeater (specifically, a dual-antenna repeater [3, Fig. 2]), focusing on the effects of the repeater on the performance of both target detection and DL communication.

In bi-static ISAC, one of the BSs transmits precoded DL data and a dedicated signal for target detection. The other BS performs joint clutter-channel and radar cross-section (RCS) estimation, and target detection, using the reflected echoes. In this setting, *ideally*, a repeater can enhance ISAC performance in two ways: (a) by amplifying the echo reflected from the target, which in turn can improve the detection performance; (b) by removing coverage-holes for the DL users.

However, the repeater also amplifies communication-to-sensing and sensing-to-communication interference. Specifically, the amplified sensing signal can incur increased interference for the communication users. Contrarily, for sensing, should the amplified DL signals (directly via the repeater) overwhelm the reflected amplified echo of the target, detection performance at the sensing receiver can severely degrade. To this end, this paper investigates these tradeoffs and discusses the *choices of precoders* at the transmit BS that can mitigate this interference while retaining the ISAC performance improvement due to the repeater. Moreover, the *developed generalized likelihood ratio test (GLRT) framework* is agnostic of the channel models and applicable to diverse propagation conditions among the repeater, BS, and users.

II. SYSTEM MODEL

We consider a bi-static ISAC system where the transmit BS, with N_t antennas, beamforms a precoded sensing signal towards a target hot-spot area while simultaneously serving K DL single-antenna users. The system also contains a dual-antenna repeater. The receiver BS, with N_r antennas, performs target detection based on the reflected echoes from the target, also via the repeater. The system model from the communication point of view is illustrated in Fig. 1a and the sensing point of view in Fig. 1b. The system entails several desired and interference channels, whose definitions are:

- $\mathbf{f}_n \in \mathbb{C}^{N_t}$: DL channel from the transmit BS to the n th user.
- $h_n \in \mathbb{C}$: channel from the transmit antenna of the repeater to the receive antenna of the n th user.
- $\mathbf{a}_t \in \mathbb{C}^{N_t}$: the channel from the transmitter to the target.
- $\mathbf{b}_t \in \mathbb{C}^{N_t}$: the channel from the transmitter to the repeater.
- $\mathbf{a}_r \in \mathbb{C}^{N_r}$: the channel from the target to the receive BS.
- $\mathbf{b}_r \in \mathbb{C}^{N_r}$: the channel from the repeater to the receive BS.
- $g \in \mathbb{C}$: the channel from the target to the repeater.
- $\mathbf{G}_B \in \mathbb{C}^{N_r \times N_t}$: the channel from the transmit to receive BS. Also, let $\hat{\mathbf{G}}_B$ and $\tilde{\mathbf{G}}_B$ be the estimate and estimation error of this direct link channel between the BSs.
- $\mathbf{C} \in \mathbb{C}^{N_r \times N_t}$: the composite clutter channel. Specifically, the clutter channel consisting of the LoS and NLoS paths caused by permanent obstacles can be measured beforehand and canceled [17]. The unknown part corresponds to the NLoS paths caused by temporary obstacles, encased in \mathbf{C} .

Apart from the clutter channel, we assume perfect channel state information (CSI) at the receiver for target detection as a necessary first step to understand the overall system performance with an intuitive and tractable formulation.² Further, let $\nu \in \mathbb{C}$ be the repeater amplification factor. The target is characterized by the associated RCS, denoted by α , which follows $\alpha \sim \mathcal{CN}(0, \sigma_\alpha^2)$, σ_α^2 being the RCS variance. The RCS is unknown at the receiver and needs to be estimated. Finally, we adopt a model wherein target detection is performed in a given hotspot, and a larger area can be covered by sending sensing signals to such hotspot areas serially [17].

III. SIGNALLING SCHEME

Let $\mathbf{x}[\tau]$ be the precoded DL transmit signal, transmitted at τ th slot, which can be written as:³

$$\mathbf{x}[\tau] = \sqrt{\rho} \left\{ \sum_{n=1}^K \sqrt{\pi_n} \mathbf{p}_n s_n[\tau] + \sqrt{\pi_T} \mathbf{p}_T s_T[\tau] \right\}, \quad \tau \in [\tau_L], \quad (1)$$

where, ρ is the total transmit power at the BS, π_n and π_T denote the fraction of the total power allocated to the n th DL user and for sensing, respectively. Also, \mathbf{p}_n and \mathbf{p}_T are the

²The composite channel via the target is $\alpha \mathbf{a}_r \mathbf{a}_t^T$. We assume only $\mathbf{a}_r \mathbf{a}_t^T$ to be known, as the BS beamforms to a specific sensing zone whose associated angle of arrival (AoA) and angle of departure (AoD) are pre-calibrated. However, α is unknown and will be estimated as a part of the GLRT later.

³All subsequent analysis is for an arbitrary subcarrier of the underlying orthogonal frequency division multiplexing (OFDM) waveform (or any monochromatic signal with a prefix to remove time-dispersion), without explicitly showing the subcarrier index, i.e., before IFFT and after FFT on the transmitter and the receiver sides; with cyclic-prefix length being larger than the maximum delay spread.

corresponding unit-normalized precoding vectors for the n th DL user and the target. Similarly, $s_n \in \mathbb{C}$ and $s_T \in \mathbb{C}$ are unit-energy, statistically independent symbols. Also, $\mathbb{E} \left[\|\mathbf{x}[\tau]\|_2^2 \right] \leq \rho$, satisfying the total transmit power budget. Finally, τ_L is the total duration over which sensing signals are transmitted, which can also be a coherence block. Given this, we can write the input-output receive (y_R^I) and transmit (y_R^O) signals at the repeater terminals as:

$$y_R^I[\tau] = \alpha g \{ \mathbf{a}_t^T \mathbf{x}[\tau] \} + \mathbf{b}_t^T \mathbf{x}[\tau], \quad (2a)$$

$$y_R^O[\tau] = \nu (y_R^I[\tau] + w_R[\tau]), \quad (2b)$$

where $w_R[\tau] \sim \mathcal{CN}(0, \sigma_R^2)$ is the additive white Gaussian noise (AWGN) at the repeater.

1) *Sensing with repeater*: The signal received at the BS is

$$\mathbf{y}_{BS}[\tau] = \alpha \mathbf{a}_r \mathbf{a}_t^T \mathbf{x}[\tau] + \mathbf{b}_r y_R^O[\tau] + \mathbf{G}_B \mathbf{x}[\tau] + \mathbf{C} \mathbf{x}[\tau] + \mathbf{w}_B[\tau],$$

where $\mathbf{w}_B[\tau] \sim \mathcal{CN}(\mathbf{0}_{N_r}, \sigma_{BS}^2 \mathbf{I}_{N_r})$ is the AWGN at the BS. Knowledge of the transmitted signal $\mathbf{x}[\tau]$ can be made available at the receiver BS via back-haul links and thus be treated as pilot symbols. Then, the receive BS can subtract $\hat{\mathbf{G}}_B \mathbf{x}[\tau]$ from \mathbf{y}_{BS} to reduce inter-BS interference. After this, substituting for y_R^O , the desired signal for the target detection and associated interference terms become:

$$\mathbf{y}_{BS}[\tau] = \mathbf{r}[\tau] \alpha + \dot{\mathbf{C}} \mathbf{x}[\tau] + \dot{\mathbf{w}}_B[\tau], \quad (3)$$

where the equivalent sensing channel $\mathbf{R}[\tau]$, equivalent clutter channel $\dot{\mathbf{C}}$, and the overall sensing noise $\dot{\mathbf{w}}_B[\tau]$, are:

$$\mathbf{r}[\tau] = (\mathbf{a}_r \mathbf{a}_t^T + \nu g \{ \mathbf{b}_r \mathbf{a}_t^T \}) \mathbf{x}[\tau], \quad (4a)$$

$$\dot{\mathbf{C}} = \mathbf{C} + \nu \mathbf{b}_r \mathbf{b}_t^T, \quad (4b)$$

$$\dot{\mathbf{w}}_B[\tau] = \tilde{\mathbf{G}}_B \mathbf{x}[\tau] + \{ \nu w_R[\tau] \} \mathbf{b}_r + \mathbf{w}_B[\tau]. \quad (4c)$$

The direct (amplified) interference due to the repeater, i.e., $\{ \nu \mathbf{b}_r \mathbf{b}_t^T \mathbf{x}[\tau] \}$, is incorporated as a part of the clutter. However, the composite channel can be pre-estimated (in LoS, it can even be fully characterized by AoAs and AoDs) to cancel this interference, similar to inter-BS interference.⁴ The resulting $\dot{\mathbf{C}} \approx \mathbf{C}$ encases the effects of environmental scatterers. Later, with (3), we will develop the target detection framework.

2) *DL communication with repeater*: For DL communication analysis, we drop the explicit dependence of index τ . The signal received at the n th DL user can be expressed as

$$y_{UE} = \mathbf{f}_n^T \mathbf{x} + h_n \{ \nu (\alpha g \{ \mathbf{a}_t^T \mathbf{x} \} + \mathbf{b}_t^T \mathbf{x} + w_R) \} + w_{UE}, \quad (5)$$

where the second term corresponds to the repeater transmission and $w_{UE} \sim \mathcal{CN}(0, \sigma_{UE}^2)$ is AWGN at the UE. Rearranging (5), we get

$$y_{UE} = (\mathbf{f}_n^T + \nu h_n \mathbf{b}_t^T) \mathbf{x} + \dot{w}_{UE}, \quad (6)$$

with $\dot{w}_{UE} = (\nu h_n w_R + w_{UE})$.

Remark 1. Note that the term " $\nu \alpha h_n g \{ \mathbf{a}_t^T \mathbf{x} \}$ " in (5) can be subsumed in the effective DL channel of the users, i.e.,

⁴This can also be cancelled by choosing the precoder for target $\left(\mathbf{I}_{N_t} - \frac{1}{\|\mathbf{b}_t\|_2^2} \mathbf{b}_t^* \mathbf{b}_t^T \right) \mathbf{a}_t$, leading to the direct link interference $\nu \mathbf{b}_r \mathbf{b}_t^T \mathbf{p}_T = 0$, where \mathbf{p}_T is the precoder intended for the target. Although it is not necessary for the subsequent analyses.

$\{\mathbf{f}_n\}$; and is therefore not explicitly shown in (6). This is because the user is agnostic of the presence of the target, and any reflection from it can be treated as from any other environmental scatterers.

IV. RCS ESTIMATION & TARGET DETECTION

Let $\bar{\mathbf{y}}_{\text{BS}} \triangleq [\mathbf{y}_{\text{BS}}^T[1], \mathbf{y}_{\text{BS}}^T[2], \dots, \mathbf{y}_{\text{BS}}^T[\tau_L]]^T \in \mathbb{C}^{N_r \times \tau_L}$ be the concatenated received signal vector at the BS at the end of the observation window. With this, we can formulate the following binary hypothesis testing framework:

$$\mathcal{H}_0: \quad \bar{\mathbf{y}}_{\text{BS}} = \bar{\mathbf{c}} + \bar{\mathbf{w}}, \quad (7a)$$

$$\mathcal{H}_1: \quad \bar{\mathbf{y}}_{\text{BS}} = \bar{\mathbf{r}} + \bar{\mathbf{c}} + \bar{\mathbf{w}}, \quad (7b)$$

where $\bar{\mathbf{r}}$, $\bar{\mathbf{c}}$, and $\bar{\mathbf{w}}$ are the concatenation of $\mathbf{r}[\tau]\alpha$, $\dot{\mathbf{C}}\mathbf{x}[\tau]$, and $\dot{\mathbf{w}}_{\text{B}}[\tau]$, respectively. The null hypothesis \mathcal{H}_0 represents the case that there is no target in the sensing area, while the alternative hypothesis \mathcal{H}_1 represents the existence of the target. The joint RCS estimation, target-free channel (i.e. clutter) estimation, and the hypothesis testing problem can be written as $\{\hat{\alpha}, \hat{\mathbf{c}}, \hat{\mathcal{H}}\} = \arg \max_{\{\alpha, \mathbf{c}, \mathcal{H}\}} p(\alpha, \mathbf{c}, \mathcal{H} | \bar{\mathbf{y}}_{\text{BS}})$, where

$\hat{\mathbf{c}} \triangleq \text{Vec}(\hat{\mathbf{C}})^5$ and $p(\alpha, \mathbf{c}, \mathcal{H} | \bar{\mathbf{y}}_{\text{BS}})$ is the joint probability density function (pdf) given the received vector $\bar{\mathbf{y}}_{\text{BS}}$. Thus, the GLRT can be formulated as $\mathcal{L} \stackrel{\mathcal{H}_0}{\geq} \lambda_s$, where

$$\mathcal{L} = \frac{\max_{\{\alpha, \mathbf{c}\}} p(\bar{\mathbf{y}}_{\text{BS}} | \alpha, \mathbf{c}, \mathcal{H}_1) p(\alpha | \mathcal{H}_1) p(\mathbf{c} | \mathcal{H}_1)}{\max_{\{\mathbf{c}\}} p(\bar{\mathbf{y}}_{\text{BS}} | \mathbf{c}, \mathcal{H}_0) p(\mathbf{c} | \mathcal{H}_0)}, \quad (8)$$

and λ_s is the threshold used by the detector, which is selected to achieve a desired false alarm probability.

Lemma 1. Let Σ_{c} and $\Sigma_{\text{s}}[\tau]$ denote the covariance of the clutter channel and the overall sensing noise $\dot{\mathbf{w}}_{\text{B}}[\tau]$ (which are individually zero mean random vectors); and let $\mathcal{J} \triangleq \ln \mathcal{L}$ be the test statistics, which evaluates to

$$\mathcal{J} = \mathbf{t}_{\mathcal{H}_1}^H \mathbf{Q}_{\mathcal{H}_1}^{-1} \mathbf{t}_{\mathcal{H}_1} - \mathbf{t}_{\mathcal{H}_0}^H \mathbf{Q}_{\mathcal{H}_0}^{-1} \mathbf{t}_{\mathcal{H}_0}, \quad (9)$$

where $\mathbf{t}_{\mathcal{H}_1}$, $\mathbf{t}_{\mathcal{H}_0}$, $\mathbf{Q}_{\mathcal{H}_0}$ are given by

$$\mathbf{t}_{\mathcal{H}_1} = \begin{bmatrix} \sum_{\tau=1}^{\tau_L} \mathbf{r}^H[\tau] \Sigma_{\text{s}}^{-1}[\tau] \mathbf{y}_{\text{BS}}[\tau] \\ \sum_{\tau=1}^{\tau_L} \mathbf{B}^H[\tau] \Sigma_{\text{s}}^{-1}[\tau] \mathbf{y}_{\text{BS}}[\tau] \end{bmatrix}, \quad (10a)$$

$$\mathbf{t}_{\mathcal{H}_0} = \sum_{\tau=1}^{\tau_L} \mathbf{B}^H[\tau] \Sigma_{\text{s}}^{-1}[\tau] \mathbf{y}_{\text{BS}}[\tau], \quad (10b)$$

$$\mathbf{Q}_{\mathcal{H}_0} = \sum_{\tau=1}^{\tau_L} \mathbf{B}^H[\tau] \Sigma_{\text{s}}^{-1}[\tau] \mathbf{B}[\tau] + \Sigma_{\text{c}}^{-1}. \quad (10c)$$

$\mathbf{Q}_{\mathcal{H}_1}$ is given in (12) on the next page, and $\mathbf{B}[\tau] \triangleq (\mathbf{x}^T[\tau] \otimes \mathbf{I}_{N_r})$. The resulting test can be evaluated as

$$\hat{\mathcal{H}} = \begin{cases} \mathcal{H}_1, & \text{if } \mathcal{J} \geq \ln \lambda'_s, \\ \mathcal{H}_0, & \text{if } \mathcal{J} < \ln \lambda'_s. \end{cases} \quad (11)$$

with $\lambda'_s (= \pi \lambda_s \sigma_{\text{T}}^2)$ being the detection threshold.

⁵“Vec(.)” stands for vectorization.

Proof. See Appendix A. ■

The complexity of the GLRT is dominated by a matrix inversion of dimension $(N_{\text{t}}N_{\text{r}} + 1) \times (N_{\text{t}}N_{\text{r}} + 1)$, and hence is $\mathcal{O}((N_{\text{t}}N_{\text{r}} + 1)^3)$. Next, only the parameter remains to be computed in the sensing noise covariance $\Sigma_{\text{s}}[\tau] = \mathbb{E}[\dot{\mathbf{w}}_{\text{B}}[\tau]\dot{\mathbf{w}}_{\text{B}}^H[\tau]]$, which is evaluated (treating transmitted symbols as pilots) as $\Sigma_{\text{s}}[\tau] = \mathbb{E}[\tilde{\mathbf{G}}_{\text{B}}\mathbf{x}[\tau]\mathbf{x}^H[\tau]\tilde{\mathbf{G}}_{\text{B}}^H] + \left\{|\nu|^2\sigma_{\text{R}}^2\right\}\mathbf{b}_{\text{r}}\mathbf{b}_{\text{r}}^H + \sigma_{\text{BS}}^2\mathbf{I}_{N_{\text{r}}}$. Next, if we assume that elements of $\tilde{\mathbf{G}}_{\text{B}}$ are independent and identically distributed (i.i.d.) $\mathcal{CN}(0, \zeta^2)$, ζ^2 capturing the power of the residual inter-BS interference [18], then $\mathbb{E}[\tilde{\mathbf{G}}_{\text{B}}\mathbf{x}[\tau]\mathbf{x}^H[\tau]\tilde{\mathbf{G}}_{\text{B}}^H]$ evaluates to $\zeta^2\|\mathbf{x}[\tau]\|_2^2\mathbf{I}_{N_{\text{r}}}$, which completes the calculation of $\Sigma_{\text{s}}[\tau]$.

Remark 2. We note that a noisy repeater can severely degrade the sensing performance, which is captured by $|\nu|^2\sigma_{\text{R}}^2$ in the sensing noise covariance. The effect of the amplified DL signals (directly via the repeater) is implicitly captured in the clutter covariance matrix in (10c).

V. DL SE ANALYSIS

In DL, based on (1) and (6), the signal received at the n th user, with $\hat{\mathbf{f}}_n \triangleq \mathbf{f}_n + \nu h_n \mathbf{b}_{\text{t}}$, can be expressed as:

$$\begin{aligned} y_{\text{UE},n} &= \sqrt{\rho}\sqrt{\pi_n}\hat{\mathbf{f}}_n^T \mathbf{p}_n s_n + \sqrt{\rho} \sum_{n'=1, n' \neq n}^K \sqrt{\pi_{n'}} \hat{\mathbf{f}}_n^T \mathbf{p}_{n'} s_{n'} \\ &\quad + \sqrt{\rho}\sqrt{\pi_{\text{T}}}\hat{\mathbf{f}}_n^T \mathbf{p}_{\text{T}} s_{\text{T}} + \dot{w}_{\text{UE}}, \end{aligned} \quad (13)$$

where the second and the third term correspond to multi-user interference and interference due to a dedicated signal for target detection. The instantaneous signal-to-interference-plus-noise ratio (SINR) at the n th DL user can then be written as

$$\text{SINR}_n = \frac{\rho\pi_n |\hat{\mathbf{f}}_n^T \mathbf{p}_n|^2}{\rho \sum_{n'=1, n' \neq n}^K \pi_{n'} |\hat{\mathbf{f}}_n^T \mathbf{p}_{n'}|^2 + \rho\pi_{\text{T}} |\hat{\mathbf{f}}_n^T \mathbf{p}_{\text{T}}|^2 + \mathbb{E}[|\dot{w}_{\text{UE}}|^2]},$$

where the noise variance can be computed as $\mathbb{E}[|\dot{w}_{\text{UE}}|^2] = \left\{|\nu|^2|h_n|^2\sigma_{\text{R}}^2 + \sigma_{\text{UE}}^2\right\}$. Next, for the choice of the precoders, the transmitter can either consider the composite channel $\{\hat{\mathbf{f}}_n\}$ or be completely agnostic of the repeater and consider $\{\mathbf{f}_n\}$. We consider regularized zero-forcing (ZF) precoding scheme for the communication user, in which case \mathbf{p}_n becomes $\mathbf{p}_n = \epsilon_n \left(\sum_{n'=1}^K \hat{\mathbf{f}}_{n'} \hat{\mathbf{f}}_{n'}^H + \zeta_{\text{ZF}} \mathbf{I}_{N_{\text{t}}}\right)^{-1} \hat{\mathbf{f}}_n$, where ϵ_n is the normalizer to ensure $\|\mathbf{p}_n\|_2^2 = 1$ and $\zeta_{\text{ZF}} > 0$ is a regularizer. For \mathbf{p}_{T} we can consider one of the following: *Target centric*: In this case, the transmitter beamforms towards the target, i.e., $\mathbf{p}_{\text{T}} = \epsilon_{\text{T}} \hat{\mathbf{f}}_{\text{T}}$, with $\hat{\mathbf{f}}_{\text{T}} = \mathbf{a}_{\text{t}}$ and ϵ_{T} is an appropriate normalizer. *Communication centric*: We null the (potentially destructive) interference from the sensing signal to the users by projecting \mathbf{p}_{T} onto the nullspace of the subspace spanned by the users' channel vectors. In this case, $\mathbf{p}_{\text{T}} = \epsilon_{\text{T}} (\mathbf{I}_{N_{\text{t}}} - \mathbf{U}\mathbf{U}^H) \hat{\mathbf{f}}_{\text{T}}$, where \mathbf{U} is a unitary matrix formed with the orthonormal columns that span the column space of $\{\hat{\mathbf{f}}_1, \hat{\mathbf{f}}_2, \dots, \hat{\mathbf{f}}_K\}$.

VI. NUMERICAL RESULTS & DISCUSSIONS

In this section, we quantify the effects of a repeater on the overall ISAC performance. The transmit power at the transmit

$$\mathbf{Q}_{\mathcal{H}_1} = \left[\begin{array}{c|c} -\frac{\sum_{\tau=1}^{\tau_c} \mathbf{r}^H[\tau] \boldsymbol{\Sigma}_s^{-1}[\tau] \mathbf{r}[\tau] + \frac{1}{\sigma_s^2}}{\left(\sum_{\tau=1}^{\tau_c} \mathbf{r}^H[\tau] \boldsymbol{\Sigma}_s^{-1}[\tau] \mathbf{B}[\tau]\right)^H} & \frac{\sum_{\tau=1}^{\tau_c} \mathbf{r}^H[\tau] \boldsymbol{\Sigma}_s^{-1}[\tau] \mathbf{B}[\tau]}{\sum_{\tau=1}^{\tau_c} \mathbf{B}^H[\tau] \boldsymbol{\Sigma}_s^{-1}[\tau] \mathbf{B}[\tau] + \boldsymbol{\Sigma}_c^{-1}} \end{array} \right] \in \mathbb{C}^{(N_t N_r + 1) \times (N_t N_r + 1)}. \quad (12)$$

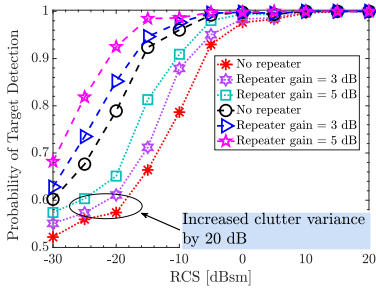


Fig. 2: Probability of detection (PoD) versus the target RCS. Here, the repeater gains are measured with respect to the noise floor at the repeater. The threshold for GLRT is adjusted to maintain a probability of false alarm (PoFA) of 0.01.

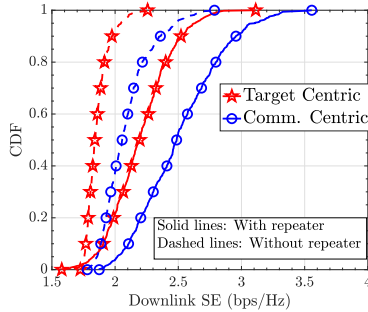


Fig. 3: Cumulative distribution function (CDF) of DL per-user SE with different choices of precoders. Equal power allocation has been employed by the transmit BS.

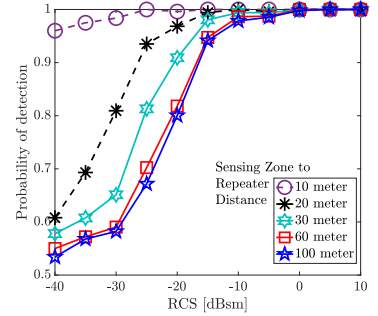


Fig. 4: Probability of detection with different repeater locations with respect to the target hotspot area. We assume the clutter variance to be 10 dB below the noise floor and the PoFA is 0.01.

BS is 1 Watt. The path loss for the communication channels is modeled using the 3GPP Urban Microcell model. Each of the BSs is equipped with 8 antennas. The height of the BS, repeaters, and users are 25, 10, and 1.5 meters, respectively, following the models adopted in [1]. The carrier frequency and bandwidth are set to 1.9 GHz and 20 MHz, respectively. At the receive BS, the noise spectral density is -174 dBm/Hz, and the noise figure is 9 dB [12]. The zone area is 500 square meters, with the BSs being in $(0, 250)$ and $(450, 250)$; the sensing zone is $(225, 250)$. The repeater is located at $(125, 250)$. The user locations are randomly generated. The repeater has the same noise power as the BS. The sensing-related parameters follow the Swerling-I model [19] and $\{\mathbf{a}_t, \mathbf{a}_r\}$ are generated following [17]. For clutter, i.i.d. Gaussian taps are assumed. Other relevant parameters are also mentioned alongside the results. The inter-BS channel and the residual interference are modeled according to [18].

Fig. 2 illustrates the effects of a repeater on the target detection. For this, the repeater is placed within 100 meters of the target hot-spot area, and we consider $K = 10$ communication users being served by the same BS, whose locations are generated uniformly at random. The slot duration for the GLRT consists of 50 channel uses, i.e. $\tau = 1, 2, \dots, 50$. For simplicity, we assume a Gaussian clutter model. Firstly, we observe that the repeater can substantially improve target detection performance as it amplifies and forwards the echo from the target and thereby improves the received echo strength at the BS. Specifically, the repeater-aided system attains a high PoD at a lower value of RCS compared to the traditional bi-static detection scenario. An increase in clutter variance degrades the overall detection performance; however, the repeater-assisted system remains robust to it in contrast with the no repeater case.

In Fig. 3 illustrates the involved trade-offs between the different choices of precoders at the transmit BS. The repeater gain is set to 5 dB above the noise floor. We can readily observe the degradation of the DL SE for the target-centric

precoder, as such a choice adds additional interference to the DL users due to the dedicated target signals, for both with and without a repeater being present in the system. Communication-centric precoder nullifies that interference. We also observe the benefits in the DL SE due to the repeater.

In Fig. 4, we illustrate the effects of moving the repeater towards the transmitter (varying the x -axis location) from the target hotspot area. This experiment reveals that a repeater near the hot-spot area can procure a high probability of detection value even for a lower target RCS. The reflected echo from a repeater, which is also further from the target, suffers severely from pathloss and contributes little to the target detection.

Finally, Fig. 5 manifests the trade-off in the ISAC performance, i.e., DL SE versus PoD/probability of missed detection (PoMD), as the repeater location is varied from a zone where DL users are located towards the target hot-spot area. Specifically, for this, we consider that 4 downlink users are randomly located within 100 meters of the transmit BS and then the repeater location (x -axis) is moved from its original location $(125, 250)$ towards the target hot-spot area. The RCS value is taken as -30 dBsm. The experiment demonstrates that a single repeater can aid communication or target detection based on its location, and thus motivates extending the current framework for a swarm-repeater-assisted system and investigating whether they can potentially offer uniformly good sensing and communication performance.

VII. REMARKS AND OPEN QUESTIONS

This paper presented initial results and a mathematical framework that facilitates repeater deployment for bi-static ISAC and reported the benefits of using a repeater in the target hot-spot area. One interesting future study is to incorporate channel estimation into the developed framework and to account for the time-varying nature of the channels. Furthermore, the impact of multiple repeaters (i.e. swarm-repeaters) in the system, including the effects of interaction between repeaters along with DL power control, can be interesting to explore.

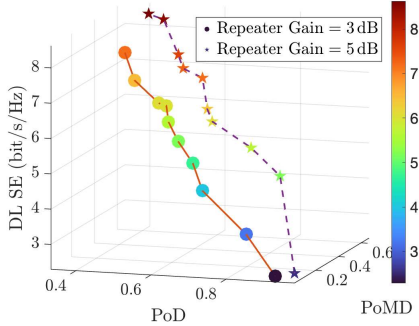


Fig. 5: DL SE versus target-detection (PoD and PoMD) performance trade-off as the repeater location is moved from user locations to target hot-spot area.

Finally note that, RISs can be a competing technology with repeaters. However, RIS and repeaters are governed by fundamentally different physics (see [3, Table I] for a detailed comparison). Notably, the repeater is a band-selective device, whereas the RIS reflects all impinging signals regardless of their frequency. Therefore, repeater-assisted systems are not subject to out-of-band interference and are compatible with operational requirements in real-world multi-operator environments. Due to their ease of deployment, repeaters are already being actively considered for standardization in multi-operator systems. The vanilla repeater does not beamform, whereas an RIS can. It remains to be investigated how an N -element RIS compares with a swarm of repeaters within a unified mathematical framework.

APPENDIX A: PROOF OF LEMMA 1

First, let us consider the optimization problem in the numerator of \mathcal{L} in (8). Recall, $\mathbf{B}[\tau] \triangleq (\mathbf{x}^T[\tau] \otimes \mathbf{I}_{N_r})$, then $\dot{\mathbf{C}}\mathbf{x}[\tau] = \mathbf{B}[\tau]\dot{\mathbf{c}}$. Further, recall that $p(\alpha|\mathcal{H}_1)$ and $p(\dot{\mathbf{c}}|\mathcal{H}_1)$ are respectively $\mathcal{CN}(0, \sigma_\alpha^2)$ and $\mathcal{CN}(\mathbf{0}_{N_r N_r}, \boldsymbol{\Sigma}_c)$. Then, because of the temporal independence of the observation vectors, the numerator of \mathcal{L} is equivalent to the following optimization

$$\begin{aligned} & \max_{\{\alpha, \dot{\mathbf{c}}\}} \left\{ \prod_{\tau=1}^{\tau_L} p(\mathbf{y}_{\text{BS}}[\tau] | \alpha, \dot{\mathbf{c}}, \mathcal{H}_1) \right\} p(\alpha | \mathcal{H}_1) p(\dot{\mathbf{c}} | \mathcal{H}_1) \\ & = \max_{\{\alpha, \dot{\mathbf{c}}\}} \left\{ \prod_{\tau=1}^{\tau_L} p(\dot{\mathbf{w}}_{\text{B}}[\tau] = \mathbf{y}_{\text{BS}}[\tau] - \mathbf{r}[\tau]\alpha + \mathbf{B}[\tau]\dot{\mathbf{c}} | \alpha, \dot{\mathbf{c}}) \right\} \\ & \quad \times p(\alpha | \mathcal{H}_1) p(\dot{\mathbf{c}} | \mathcal{H}_1) \\ & = \mathcal{C}_{\mathcal{H}_1} \exp \left\{ - \min_{\{\alpha, \dot{\mathbf{c}}\}} f(\alpha, \dot{\mathbf{c}}; \mathcal{H}_1) \right\}, \end{aligned}$$

where $\mathcal{C}_{\mathcal{H}_1}$ is a constant and the function $f(\alpha, \dot{\mathbf{c}}; \mathcal{H}_1)$, after some algebra, can be expressed as

$$\sum_{\tau=1}^{\tau_L} \mathbf{y}_{\text{BS}}^H[\tau] \boldsymbol{\Sigma}_s^{-1}[\tau] \mathbf{y}_{\text{BS}} + \mathbf{z}^H \mathbf{Q}_{\mathcal{H}_1} \mathbf{z} - 2\Re\{\mathbf{z}^H \mathbf{t}_{\mathcal{H}_1}\},$$

where $\mathbf{z} = [\alpha, \dot{\mathbf{c}}^T]^T$ and the positive semi-definite (PSD) matrix $\mathbf{Q}_{\mathcal{H}_1}$ has the block-structure as shown in (12). Then, $\mathbf{t}_{\mathcal{H}_1}$ is expressed as shown in (10a). Now, the estimate of \mathbf{z} obtained from $f(\alpha, \dot{\mathbf{c}}; \mathcal{H}_1)$ equals to $\mathbf{Q}_{\mathcal{H}_1}^{-1} \mathbf{t}_{\mathcal{H}_1}$, resulting

$$- \min_{\{\alpha, \dot{\mathbf{c}}\}} f(\alpha, \dot{\mathbf{c}}; \mathcal{H}_1) = - \sum_{\tau=1}^{\tau_L} \mathbf{y}_{\text{BS}}^H[\tau] \boldsymbol{\Sigma}_s^{-1}[\tau] \mathbf{y}_{\text{BS}} + \mathbf{t}_{\mathcal{H}_1}^H \mathbf{Q}_{\mathcal{H}_1}^{-1} \mathbf{t}_{\mathcal{H}_1}.$$

Similarly, we can solve the optimization of the denominator of \mathcal{L} , and show that it evaluates to

$$\begin{aligned} & \max_{\{\dot{\mathbf{c}}\}} p(\bar{\mathbf{y}}_{\text{BS}} | \dot{\mathbf{c}}, \mathcal{H}_0) p(\dot{\mathbf{c}} | \mathcal{H}_0) \\ & = \mathcal{C}_{\mathcal{H}_0} \exp \left\{ \mathbf{t}_{\mathcal{H}_0}^H \mathbf{Q}_{\mathcal{H}_0}^{-1} \mathbf{t}_{\mathcal{H}_0} - \sum_{\tau=1}^{\tau_L} \mathbf{y}_{\text{BS}}^H[\tau] \boldsymbol{\Sigma}_s^{-1}[\tau] \mathbf{y}_{\text{BS}} \right\}, \end{aligned}$$

where $\mathcal{C}_{\mathcal{H}_0}$ is a constant, $\mathbf{t}_{\mathcal{H}_0}$ and $\mathbf{Q}_{\mathcal{H}_0}$ are respectively given by (10b) and (10c). From the above, we get the final result. ■

REFERENCES

- [1] J. Bai *et al.*, "Repeater swarm-assisted cellular systems: Interaction stability and performance analysis," *IEEE Trans. Wireless Commun.*, vol. 25, pp. 10018–10034, 2026.
- [2] E. G. Larsson *et al.*, "Reciprocity calibration of dual-antenna repeaters," *IEEE Wireless Commun. Lett.*, vol. 13, no. 6, pp. 1606–1610, Jun. 2024.
- [3] S. Willhammar *et al.*, "Achieving distributed MIMO performance with repeater-assisted cellular massive MIMO," *IEEE Commun. Mag.*, vol. 63, no. 3, pp. 114–119, Mar. 2025.
- [4] C.-K. Wen *et al.*, "Shaping a smarter electromagnetic landscape: IAB, NCR, and RIS in 5G standard and future 6G," *IEEE Commun. Stand. Mag.*, vol. 8, no. 1, pp. 72–78, Mar. 2024.
- [5] K. Dong *et al.*, "Network-controlled repeater aided time-sensitive communications in urban vehicular networks," *IEEE Wireless Commun. Lett.*, vol. 14, no. 5, pp. 1511–1515, May 2025.
- [6] O. A. Topal *et al.*, "Fair and energy-efficient activation control mechanisms for repeater-assisted massive MIMO," in *Proc. 23rd Int. Symp. Model. Optim. Mobile, Ad Hoc, Wireless Netw. (WiOpt)*, May 2025, pp. 1–7.
- [7] M. Åström *et al.*, "RIS in cellular networks – challenges and issues," 2024. [Online]. Available: <https://arxiv.org/abs/2404.04753>
- [8] 3GPP, "New WID on NR network-controlled repeaters," 3rd Generation Partnership Project (3GPP), RP 222673, Sep. 2022, TSG RAN meeting no. 97-e. [Online]. Available: https://www.3gpp.org/ftp/tsg_ran/TSG_RAN/TSGR_97e/Docs/RP-222673.zip
- [9] A. Kaushik *et al.*, "Toward integrated sensing and communications for 6G: Key enabling technologies, standardization, and challenges," *IEEE Commun. Standards Mag.*, vol. 8, no. 2, pp. 52–59, June 2024.
- [10] X. Zhu *et al.*, "Enabling intelligent connectivity: A survey of secure ISAC in 6G networks," *IEEE Commun. Surveys Tuts.*, vol. 27, no. 2, pp. 748–781, Apr. 2025.
- [11] J. A. Zhang *et al.*, "Enabling joint communication and radar sensing in mobile networks—a survey," *IEEE Commun. Surveys Tuts.*, vol. 24, no. 1, pp. 306–345, Firstquarter 2022.
- [12] M. Elfiatoure *et al.*, "Multiple-target detection in cell-free massive MIMO-assisted ISAC," *IEEE Trans. Wireless Commun.*, vol. 24, no. 5, pp. 4283–4298, May 2025.
- [13] B. He *et al.*, "Bistatic-enhancement MIMO ISAC: Joint beamforming design in cell-free communication and bistatic radar systems," *IEEE Trans. Wireless Commun.*, pp. 1–1, 2025.
- [14] X. Shen *et al.*, "Fundamental tradeoff of bistatic ISAC under Gaussian fading channels at finite blocklength," *IEEE Trans. Inf. Theory*, pp. 1–1, 2025.
- [15] A. Bazzi *et al.*, "Low dynamic range for RIS-aided bistatic integrated sensing and communication," *IEEE J. Sel. Areas Commun.*, vol. 43, no. 3, pp. 912–927, Mar. 2025.
- [16] H. Åkesson *et al.*, "Impact of network-controlled repeaters in integrated sensing and communication systems," in *Proc. 33rd IEEE Eur. Signal Process. Conf.*, Sep. 2025, pp. 1010–1014.
- [17] Z. Behdad *et al.*, "Multi-static target detection and power allocation for integrated sensing and communication in cell-free massive MIMO," *IEEE Trans. Wireless Commun.*, vol. 23, no. 9, pp. 11580–11596, Sep. 2024.
- [18] A. Chowdhury *et al.*, "Half-duplex APs with dynamic TDD versus full-duplex APs in cell-free systems," *IEEE Trans. Commun.*, vol. 72, no. 7, pp. 3856–3872, Jul. 2024.
- [19] Z. Wei *et al.*, "Integrated sensing and communication channel modeling: A survey," *IEEE Internet Things J.*, vol. 12, no. 12, pp. 18850–18864, Jun. 2025.